



HAL
open science

Spectroscopy of the electronic states of the Heusler compounds Co_2FeAl and $\text{Co}_2\text{Cr}_{0.6}\text{Fe}_{0.4}\text{Al}$ and the influence of oxidation

Martin Jourdan, Fabian Grosse-Schulte, Michaela Hahn, Gerd Schönhense

► **To cite this version:**

Martin Jourdan, Fabian Grosse-Schulte, Michaela Hahn, Gerd Schönhense. Spectroscopy of the electronic states of the Heusler compounds Co_2FeAl and $\text{Co}_2\text{Cr}_{0.6}\text{Fe}_{0.4}\text{Al}$ and the influence of oxidation. *Journal of Physics D: Applied Physics*, 2011, 44 (15), pp.155001. 10.1088/0022-3727/44/15/155001 . hal-00609757

HAL Id: hal-00609757

<https://hal.science/hal-00609757>

Submitted on 20 Jul 2011

HAL is a multi-disciplinary open access archive for the deposit and dissemination of scientific research documents, whether they are published or not. The documents may come from teaching and research institutions in France or abroad, or from public or private research centers.

L'archive ouverte pluridisciplinaire **HAL**, est destinée au dépôt et à la diffusion de documents scientifiques de niveau recherche, publiés ou non, émanant des établissements d'enseignement et de recherche français ou étrangers, des laboratoires publics ou privés.

Spectroscopy of the electronic states of the Heusler compounds Co_2FeAl and $\text{Co}_2\text{Cr}_{0.6}\text{Fe}_{0.4}\text{Al}$ and the influence of oxidation

Martin Jourdan, Fabian Große-Schulte, Michaela Hahn, and Gerd Schönhense

Institut für Physik, Johannes Gutenberg-Universität, Staudinger Weg 7, 55128 Mainz, Germany

E-mail: jourdan@uni-mainz.de

Abstract. The band structures of the Heusler compounds $\text{Co}_2\text{Cr}_{0.6}\text{Fe}_{0.4}\text{Al}$ and Co_2FeAl were investigated in-situ by angle resolved ultraviolet photoemission spectroscopy (ARUPS). The samples were prepared by a sputtering process optimized for tunneling junction preparation, the photoemission process in normal direction of the (001)-oriented thin films was excited by a Helium gas discharge lamp ($h\nu = 21.2\text{eV}$ and $h\nu = 40.8\text{eV}$). The spectra of clean samples are compared with calculations of the total and partial bulk density of states and are evaluated within the three-step model of photoemission. Basic agreement with theoretical predictions of the bulk band structure is concluded. At oxygen exposures of the thin films of only 1 Langmuir a chemisorption phase with significant changes of the valence-band spectrum near the Fermi-energy is observed. At 10L oxygen the spectra are indicative of an oxide within the UPS probing depth.

1. Introduction

Band structure calculations, which predict half metallic properties for several Heusler compounds [1, 2, 3], initiated great experimental efforts concerning this class of materials. Such materials with a spin polarization at the Fermi energy close to 100% are highly desirable for spintronics applications. The validation of the calculated electronic properties remains difficult, though. These materials with medium strong electronic correlations provide a test for modern band structure calculation methods.

The preparation and investigation of planar magnetic tunneling junctions is one method which allows conclusions concerning the spin polarization and electronic density of states (DOS) near the Fermi energy (e. g. [4, 5, 6, 7, 8]). Another technique, which is in principle more powerful concerning the accessible energy range and directional sensitivity, is angle resolved photoemission spectroscopy (ARPES). However, ARPES is extremely surface sensitive and the preparation of Heusler compounds with clean and well ordered surface for such measurements poses a major challenge. Valence band spectroscopy is usually performed on bulk samples which are fractured or polished inside the spectroscopy chamber (e. g. [9, 10, 11]). Another approach is a sequence of sputter cleaning and annealing processes of a bulk or thin film sample (often capped with a protection layer) after ex-situ transfer into an analysis chamber [12, 13]. If complex intermetallic alloys like the Heusler compounds are investigated, all these preparation methods result in more or less distorted surface order and stoichiometry. In order to deal with this problem, hard x-ray photoemission spectroscopy (HAXPES) is employed, which is able to detect photoemitted electrons from Heusler thin films capped by a thin MgO layer (e. g. [14, 15]). Alternatively, uncapped Heusler thin films (grown by Pulsed Laser Deposition) were transported in a vacuum suitcase from the preparation chamber to a synchrotron facility for spin resolved photoemission spectroscopy [16].

Here, a different approach is presented: Uncapped Heusler thin films were prepared by a process optimized for tunneling junction preparation and were investigated in-situ by angle resolved ultraviolet photoemission spectroscopy (ARUPS). Thus it is possible to study undistorted atomically clean Heusler surfaces and the results can be related directly to our work on Heusler based tunneling junctions [5, 6]. Our main intention is the identification of intrinsic band structure related features in the ARUPS data, which can be used to test the predictions of band structure calculations. By controlled oxidation of the samples, degradation related features in the spectra are distinguishable from intrinsic properties of the Heusler compounds.

The Heusler compounds $\text{Co}_2\text{Cr}_{0.6}\text{Fe}_{0.4}\text{Al}$ and Co_2FeAl were investigated. The spin polarization of the former is predicted to be close to 100%, whereas in the case of the latter theory yields a reduced value [18, 17].

2. Experiment

Epitaxial Heusler thin films were prepared by rf-magnetron sputtering from stoichiometric targets on MgO(100) substrates at room temperature. The sputtering chamber is part of an Omicron Molecular Beam Epitaxy (MBE)-/sputtering-/analysis-cluster. The base pressure of the sputtering chamber was $\simeq 2 \times 10^{-9}$ mbar. 6N purity Argon flowing through a cleaning cartridge (Linde Oxisorb), which is specified to reduce the amount of oxygen to <5 ppb, was used as sputtering gas at 0.1mbar. The thin films show epitaxial B2 order already as deposited. Subsequent annealing at 550°C for 15 minutes in an MBE chamber improves the structural and morphological order (formation of terraces) of the thin film. The base pressure of the MBE annealing chamber amounts to $\simeq 1 \times 10^{-10}$ mbar, this pressure increases up to $\simeq 2 \times 10^{-9}$ mbar at maximum annealing temperature, the total time in the annealing chamber was 75 minutes. For additional details on the sample preparation and structural characterization (x-ray diffraction, electron diffraction, in-situ scanning tunneling microscopy), see [6, 19]. The surface magnetic moments of the $\text{Co}_2\text{Cr}_{0.6}\text{Fe}_{0.4}\text{Al}$ and Co_2FeAl thin films are identical with the bulk moments as determined by x-ray magnetic circular dichroism experiments (TEY- and TM-XMCD) and amount to $3.5\mu_{\text{B}}$ /f. u. and $4.8\mu_{\text{B}}$ /f. u., respectively [20, 21].

In-situ ARUPS is performed in a special analysis chamber (base pressure $\simeq 5 \times 10^{-10}$ mbar) which is part of the UHV-cluster. We use a Leybold EA-10/100 hemispherical electron energy analyzer and a Helium gas discharge lamp, which produces unpolarized photons with energies of 21.2eV (He I) and 40.8eV (He II). The diameter of the visible spot amounts to $\simeq 3$ mm. During operation of the gas discharge lamp the He partial pressure in the analysis chamber is $\simeq 6 \times 10^{-8}$ mbar. The photon angle of incidence on the sample surface was $\simeq 50^\circ$. The sample can be tilted with a maximum angle of 20° off-normal (the photon angle of incidence thereby changes to $\simeq 70^\circ$), the angular resolution of the energy analyzer is 6° . The set-up does not allow the comparison of absolute photoemission intensities of different samples or of samples transferred between measurements into other chambers. All ARUPS curves shown for comparison in one graph are scaled.

As concluded from the width of the Fermi edge of a silver thin film, the energy resolution of our ARUPS set-up amounts to $\simeq 200$ meV.

In order to study the effect of oxidation on the Heusler thin films, the samples were exposed to small amounts of oxygen. In an additional chamber, which is part of the UHV-cluster, an oxygen flow resulting in a pressure of 1×10^{-6} mbar (hot cathode gauge) was adjusted. The thin film to be oxidized was positioned directly in front a closed gate valve (size CF-100), which connects the UPS chamber (with running Ion-Getter- and Turbopumps) with the oxygen filled chamber. After opening the gate valve the pressure gauge showed immediately a value of 2×10^{-7} mbar, which remained constant for the typical exposure times of the order of 10s. The oxidation was ended by closing the gate valve again.

3. The influence of oxidation

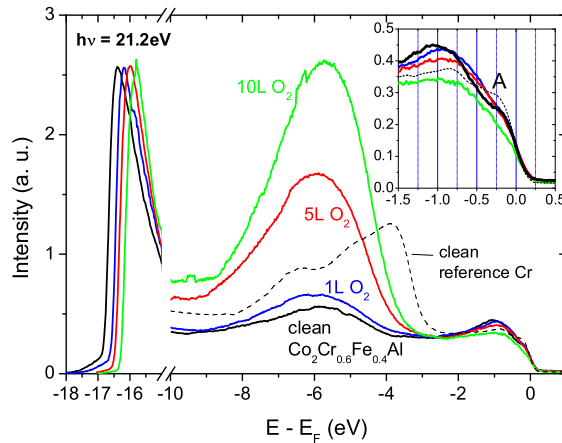


Figure 1. Comparison of the ARUPS spectra ($h\nu = 21.2\text{eV}$) of a clean $\text{Co}_2\text{Cr}_{0.6}\text{Fe}_{0.4}\text{Al}$ thin film (black line), after exposure to $\simeq 1\text{L O}_2$ (blue line), to $\simeq 5\text{L O}_2$ (red line) and to $\simeq 10\text{L O}_2$ (green line). Additionally, the ARUPS spectrum of a clean Cr thin film is shown as a reference (dashed thin line). The inset shows the spectra near E_F in more detail.

The combination of sputter deposition (typical method for Heusler thin film growth) and in-situ ARUPS has not been used yet. In order to demonstrate the feasibility of sufficient surface purity, first a most reactive Chromium (100) thin film prepared by exactly the same process as described above for the Heusler compounds, including the annealing step, was studied (dashed line in Fig. 1). The ARUPS spectrum is in good agreement with published data obtained on MBE grown Cr thin films [22, 23] with one additional feature at $\simeq -6.5\text{eV}$, which can be attributed to weak oxidation with $\simeq 1$ Langmuir (L) O_2 [24]. Thus it was demonstrated that the combination of sputter deposition, annealing and ARUPS processes is able to produce the intrinsic features of highly reactive transition metals such as the Heusler compounds. As shown below, the Heusler samples prepared without controlled exposure to oxygen show at the utmost weak traces of oxidation. Those samples are called *clean* in the following.

The influence of intended oxidation on the ARUPS spectra of the Heusler compound $\text{Co}_2\text{Cr}_{0.6}\text{Fe}_{0.4}\text{Al}$ was investigated. For both excitation energies $h\nu=21.2\text{eV}$ (Fig. 1, solid lines) and $h\nu=40.8\text{eV}$ (Fig. 2) increasing oxidation of the thin film produces a growing emission peak at $E - E_F \simeq -6\text{eV}$ and a decreasing relative intensity at higher energies. The broad $\simeq -6\text{eV}$ signal is thus indicative for the oxidation of the Heusler compound. In both figures the data was scaled to show the same intensity at $E - E_F = 2.5\text{eV}$.

Furthermore, some characteristic features in the spectra of clean samples (labeled A in the inset of Fig. 1 and E and H in Fig. 2), are already quenched by the exposure of the samples to only 1L of oxygen. Recently it was shown for Fe(001), that a surface coverage by a single layer of oxygen produces additional states at E_F [25]. A similar mechanism could explain the quenching of the features A and E in the case of $\text{Co}_2\text{Cr}_{0.6}\text{Fe}_{0.4}\text{Al}$.

This sensitivity of the Heusler compound to oxidation is highly relevant for the

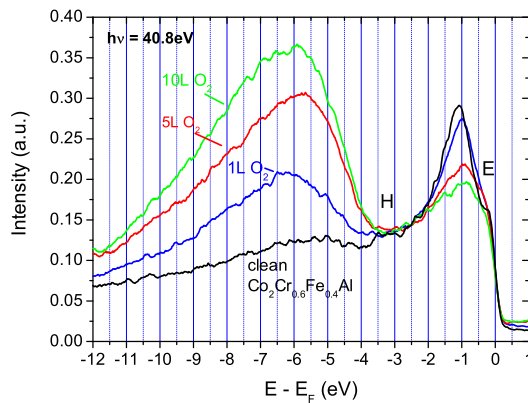


Figure 2. Comparison of the ARUPS spectra ($h\nu = 40.8\text{eV}$) of a clean $\text{Co}_2\text{Cr}_{0.6}\text{Fe}_{0.4}\text{Al}$ thin film (black line), after exposure to $\simeq 1\text{L O}_2$ (blue line), to $\simeq 5\text{L O}_2$ (red line) and to $\simeq 10\text{L O}_2$ (green line).

preparation of magnetic tunneling junctions. It explains the experimental observation that over-oxidation of the tunneling barrier or aging of the Heusler surface is a major problem if $\text{Co}_2\text{Cr}_{0.6}\text{Fe}_{0.4}\text{Al}$ or similar compounds are used as tunneling electrodes. In our previous experiments on $\text{Co}_2\text{Cr}_{0.6}\text{Fe}_{0.4}\text{Al}/\text{AlO}_x/\text{CoFe}$ tunneling junctions we demonstrated that slightly aged $\text{Co}_2\text{Cr}_{0.6}\text{Fe}_{0.4}\text{Al}$ surfaces produce only half of the magnetoresistance of junctions prepared with optimized conditions [6].

In ARUPS, the high reactivity of $\text{Co}_2\text{Cr}_{0.6}\text{Fe}_{0.4}\text{Al}$ with oxygen is also demonstrated by the increase of the work function $e\Phi$ as determined from the lengths of the spectra (Fig. 1) [27]. Whereas $e\Phi = 4.5\text{eV}$ for clean samples, it increases to 4.8eV , if the thin film was exposed to 1L of oxygen (5.1eV for 10L).

The 1L spectrum corresponds to a chemisorption phase of oxygen with a rather small but significant influence on the near Fermi region. The 10L oxygen spectrum reveals beginning bulk oxidation with loss of metallicity within the UPS probing depth as evident from the disappearance of the Fermi-cutoff in Figs. 1 and 2. The relative emission intensity of the oxygen state (2p-like) referred to the Heusler states (3d-like) is reduced for $h\nu = 40.8\text{eV}$ compared to $h\nu = 21.2\text{eV}$. This is due to the different energy dependence of the photoionisation cross sections [26]. All features due to direct transition (see section V) are quenched by the exposure of the thin films to 10L oxygen for both excitation energies.

In ref. [6] we showed by in-situ scanning tunneling microscopy how aging the $\text{Co}_2\text{Cr}_{0.6}\text{Fe}_{0.4}\text{Al}$ thin films in moderate vacuum conditions results in a modified morphology of AlO_x tunneling barriers deposited on top of the samples. The concluded change of the surface chemistry by aging of the Heusler thin films is consistent with the pronounced sensitivity to oxidation as observed by ARUPS.

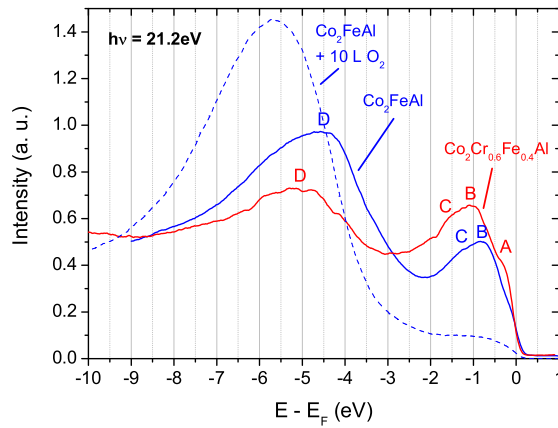


Figure 3. Comparison of the ARUPS spectra ($h\nu = 21.2 \text{ eV}$) of a $\text{Co}_2\text{Cr}_{0.6}\text{Fe}_{0.4}\text{Al}$ thin film (red line) and a Co_2FeAl thin film (blue line). The dashed curve shows the spectrum measured on the Co_2FeAl sample after oxidation with 10L O_2 for comparison.

4. ARUPS on clean samples and Density of States

Figs. 3 and 4 compare the ARUPS spectra of the two compounds $\text{Co}_2\text{Cr}_{0.6}\text{Fe}_{0.4}\text{Al}$ and Co_2FeAl excited by $h\nu = 21.2 \text{ eV}$ and $h\nu = 40.8 \text{ eV}$ photons.

It should be considered that ARUPS is very surface sensitive (electron mean free path $0.4 - 1 \text{ nm}$ [28]) and that in normal emission from the (001) oriented thin films, assuming an $L2_1$ structure, only the electronic states with momentum k parallel to the Γ -X direction contribute. However, only moderate DOS anisotropies are expected for cubic crystal structures. Within the usual three-step model of photoemission (ARUPS spectra dominated by direct optical transitions), the intensity is related to a joint density of an initial and a final electronic state [28] (see section V). Nevertheless, emission peaks should always be related to an energy range with a high density of initial states.

The most obvious differences in the ARUPS spectra of $\text{Co}_2\text{Cr}_{0.6}\text{Fe}_{0.4}\text{Al}$ and Co_2FeAl are observed near the Fermi edge, which is well developed for both compounds. In the case of $\text{Co}_2\text{Cr}_{0.6}\text{Fe}_{0.4}\text{Al}$ clear shoulder-like features (labeled A for $h\nu = 21.2 \text{ eV}$, Fig. 3, and E for $h\nu = 40.8 \text{ eV}$, Fig. 4) are observed on the rising edge of pronounced emission peaks (labeled B and F) at -1.1 eV . In the case of Co_2FeAl an emission peak (labeled B and F) without any shoulder on its edge is observed at -0.85 eV .

This difference between the two compounds can be related to features of the theoretical (FLAPW-GGA) bulk total density of states (TDOS) as published by G.H. Fecher et al. [17]. Fig. 5 shows the TDOS of the two Heusler compounds with the $L2_1$ structure as derived from a digitized spin resolved graph of ref. [17]. Disorder on the Cr,Fe - Al sites (B2 structure) is in general expected to result in a smearing out of the DOS [18]. In the calculation there is a pronounced peak in the DOS of $\text{Co}_2\text{Cr}_{0.6}\text{Fe}_{0.4}\text{Al}$ (labeled A/E in Fig. 5), which does not exist for Co_2FeAl . We account this peak to the origin of the feature A/E in the ARUPS data. Also the features B/F and

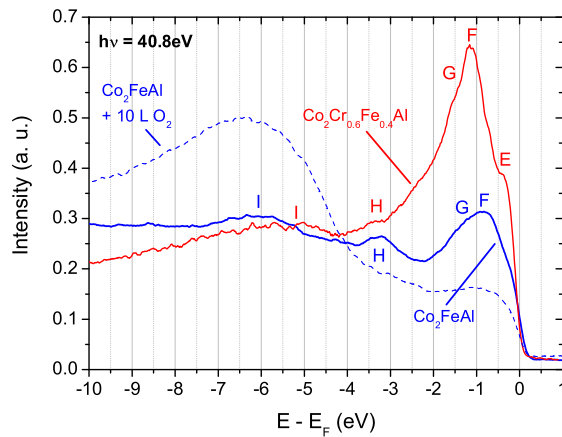


Figure 4. Comparison of the ARUPS spectra ($h\nu = 40.8\text{eV}$) of a $\text{Co}_2\text{Cr}_{0.6}\text{Fe}_{0.4}\text{Al}$ thin film (red line) and a Co_2FeAl thin film (blue line). The dashed curve shows the spectrum measured on the Co_2FeAl sample after oxidation with 10L O_2 for comparison.

C/G of the experimental ARUPS data can be identified in the theoretical TDOS. This good agreement between experiment and theory is consistent with our observation of a relatively large tunneling magnetoresistance of $\text{Co}_2\text{Cr}_{0.6}\text{Fe}_{0.4}\text{Al}/\text{AlO}_x/\text{CoFe}$ junctions (101%), which is, again in agreement theory, evidence for a large spin polarization of this Heusler compound [6]. For Co_2FeAl the position of the Fermi energy has to be shifted by $\simeq -0.15\text{eV}$ in the theoretical data in order to be consistent with the ARUPS data. Considering that the exact determination of the position of the Fermi energy poses a challenge for band structure calculations, the agreement with the experimental results is relatively good. However, such a shift moves the Fermi energy toward the edge of the minority pseudo band gap in the calculation by G.H. Fecher et al. [17] and thus is reducing the spin polarization. This is in accordance with our observation of only a small tunneling magnetoresistance of $\text{Co}_2\text{FeAl}/\text{AlO}_x/\text{CoFe}$ junctions (34%).

At $h\nu = 21.2\text{eV}$, a broad emission maximum (labeled D) is observed at -5.0eV for $\text{Co}_2\text{Cr}_{0.6}\text{Fe}_{0.4}\text{Al}$ and at -4.6eV for Co_2FeAl . These maxima are at energies not identical with the energies at which the oxidation derived peaks discussed in section III are observed (Fig. 1 and Fig. 3). However, they are close and it cannot be excluded that feature D is related to beginning sample oxidation. At these energies, no peaks in the bulk densities of states were calculated for both compounds [18, 17, 9, 30], but, as we will show in section V, these peaks could be generated by direct transitions into a free electron-like parabolic band.

Alternatively, a recent publication on the surface DOS (3-unit cell slab) obtained a peak in the relevant energy range for Co_2FeAl [31]. The same publication shows that the other DOS features remain qualitatively unchanged in the surface region as compared to the bulk.

With a photon energy of $h\nu = 40.8\text{eV}$, another clear emission maximum (labeled H)

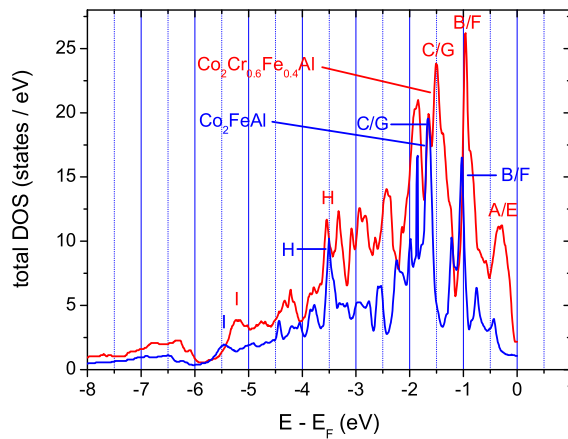


Figure 5. Total density of states of $\text{Co}_2\text{Cr}_{0.6}\text{Fe}_{0.4}\text{Al}$ and Co_2FeAl as derived from a digitized graph from G.H. Fecher et al. [17]. Disorder on the Cr,Fe - Al sites (B2 structure) is in general expected to result in a smearing out of the density of states [18].

is seen at -3.3eV for Co_2FeAl , which is also present but less distinct for $\text{Co}_2\text{Cr}_{0.6}\text{Fe}_{0.4}\text{Al}$. Again, this feature can be related to a maximum in the calculated bulk TDOS of the two compounds (Fig. 5), which appears in theory at slightly lower energies.

One more emission maximum is visible at $\simeq -6\text{eV}$ ($h\nu = 40.8\text{eV}$, labeled I). This maximum may be related to sample oxidation, because its position is identical with the position of a huge peak which grows upon exposure of the thin films to oxygen. On the other hand, it could as well be related to the bulk band structure of the Heusler compounds as will be shown below.

5. Free electron final state model

The most simple assumption of the final state within the three-step model is that of a free electron (e. g. [32]), which was used successfully e. g. for the analysis of ARUPS data measured on Cr [22, 23]. Within this model, the final state is described by a free electron-like parabolic band

$$E_f(\mathbf{k}) = \hbar^2 \mathbf{k}^2 / 2m + V_0, \quad (1)$$

where the only free parameter is V_0 , the bottom of a muffin tin potential referenced to the Fermi energy. We only apply this model to the compound Co_2FeAl , for which more detailed band structure calculations are published.

In the calculated band structure of Co_2FeAl [30], a free electron-like dispersion branch along the Γ -X direction is clearly visible (see Fig. 6). We take the bottom of this dispersion branch to determine $V_0 = -9.8\text{eV}$ for the final state dispersion. In ref. [30] and Fig. 6 it is clearly visible that due to interactions with d-electron states the free electron-like dispersion is not simply folded back into the first Brillouin zone

at energies close to E_F . However, this is not relevant for our final state model because we intend to describe photoexcited electronic states well above the Fermi energy. Also due to their high energy those states are expected to show a substantial broadening of $\simeq 2\text{-}3\text{eV}$ [32]. From the assumption of free electron-like final states follows a one-to-one correspondence between the energy of the emitted photoelectrons E_{kin} and the momentum of the electronic states parallel to the Γ -X direction $k_{\Gamma-X}$ ($e\Phi$: work function, E_i : initial state energy):

$$\begin{aligned} (\hbar k_{\Gamma-X})^2 &= 2m(E_f - V_0) = 2m(E_{kin} + e\Phi - V_0) \\ &= 2m(E_i + h\nu - V_0) \end{aligned}$$

In Fig. 6 the final state free electron parabola as described above is plotted in the first Brillouin zone of the $L2_1$ unit cell along the Γ -X direction ($|\Gamma - X| = 2\pi/a = 1.01\text{\AA}^{-1}$). The initial state energies are determined from the positions of the ARUPS emission peaks of Co_2FeAl . The direct transitions due to the absorption of photons are indicated by vertical arrows, the positions of the transitions on the momentum-axis were calculated by the formula given above. It is obvious that this simple parameter-free model for the description of the photoemission processes results in a consistent description of the experimental data.

The experimental data is compared with a band structure calculation by G. H. Fecher and C. Felser [30], in which they employ the same method as in [17], but show dispersion branches over a relatively wide energy region below E_F . In Fig. 6 the digitized part of the spin resolved band structure for Co_2FeAl along the Γ -X direction is taken from a graph of [30] and amended by a free electron-like dispersion branch as described above.

The initial states of the ARUPS emission maxima B/F and C/G appear just above very flat theoretical dispersion branches. The same applies to the emission maximum H. As already proposed above, the experimental data indicates that the position of the Fermi energy in the calculation should be shifted by $\Delta E \simeq -0.15\text{eV}$.

The experimentally derived data from transition D is also positioned on a branch of the dispersion, but this branch shows a pronounced slope resulting in a small DOS. It is possible that the mechanism of a direct transition into the final state band produces this experimentally observed emission maximum as well. However, due to its distinctiveness beginning oxidation or a specific surface DOS [31] as discussed in section III seems a more likely origin. Also in section IV some evidence was given, that the emission maximum I may be associated with sample oxidation. From Fig. 6 it could be concluded that this emission maximum is generated by the flat band region close to the X-point, but this interpretation would not be consistent with the for all other transitions necessary shift of E_F . Nevertheless, in this sense it could be associated with the upper edge of the local gap at X in the band structure.

Another band structure calculation from the same publication [30], derived with the LDA+U method, shows inferior agreement.

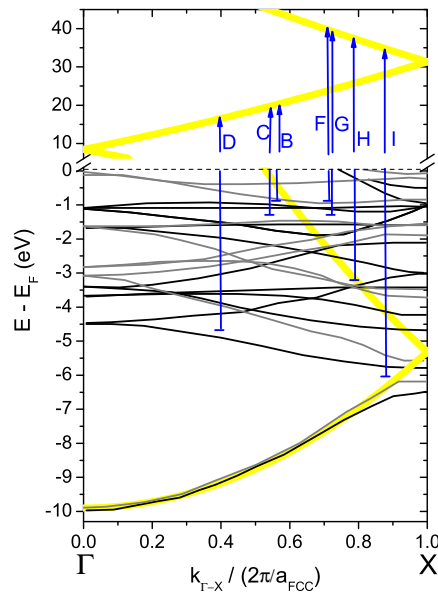


Figure 6. Calculated bulk dispersion branches of Co_2FeAl parallel to the Γ - X direction digitized from a graph of G. H. Fecher and C. Felser [30] amended by a free electron-like final state dispersion branch (wide yellow lines). The thin black lines indicate the majority branches and the thin gray lines the minority branches. The experimentally observed ARUPS transitions are indicated by blue arrows. The labels provide the assignment to the emission peaks of Figs. 3 and 4.

Additional data can be collected in principle by tilting the sample with respect to the analyzer (e. g. [32]). In our experiments no shift of the emission peak positions was observed by tilting by the maximum possible angle of 20° . Such a behavior should be expected because this tilt changes $k_{\Gamma-X}$ only by $0.08|\Gamma - X|$ (for transition B), which, considering the flatness of the dispersion branches, does not result in a significant energy shift.

In the ARUPS data analysis the dipole selection rules for direct optical transitions (e. g. [28]) are not considered. Except for the lowest energy band (sp-like), all bands shown in Fig. 6 are mainly of d-character. For unpolarized photons with an angle of incidence of $\simeq 50^\circ$ we thus expect that all transitions discussed above are allowed. However, the data analysis would be more reliable if a DOS calculation weighted by scattering cross sections was available.

6. Summary

By the combination of thin film deposition techniques optimized for tunneling junction preparation and in-situ ARUPS experiments intrinsic band structure properties of Heusler materials can be investigated. Employing two emission lines of a Helium

gas discharge lamp, photoemission spectra of the Heusler compounds $\text{Co}_2\text{Cr}_{0.6}\text{Fe}_{0.4}\text{Al}$ and Co_2FeAl were measured. These spectra show different characteristic features in agreement with the predictions of band structure calculations. The spectra show several energy dependent intensity maxima which can be analyzed within the three-step model of photoemission assuming a free electron-like final state. The experimental results for Co_2FeAl were compared in detail with a theoretical bulk band structure. Good agreement was demonstrated taking into account a small shift of the Fermi energy.

Characteristic ARUPS features due to sample oxidation could be identified. The extreme chemical reactivity is obvious from spectra taken at different oxygen dosage. At only 1L the O_2 derived ARUPS spectrum close to E_F changes significantly. At 10L the onset of oxidation leads to a quenching of the spectral features close to E_F .

References

- [1] de Groot R A, Mueller F M, van Engen P G, and Buschow K H J 1983 *Phys. Rev. Lett.* **50** 2024
- [2] Galanakis I 2002 *J. Phys.: Condens. Matter* **14** 6329
- [3] Picozzi S, Continenza A, Freeman A J 2002 *Phys. Rev. B* **66** 094421
- [4] Sakuraba Y, Miyakoshi T, Oogane M, Ando Y, Sakuma A, Miyazaki T, and Kubota H 2006 *Appl. Phys. Lett.* **89** 052508
- [5] Jourdan M, Conca A, Herbort C, Kallmayer M, Elmers H J, and Adrian H 2007 *J. Appl. Phys.* **102** 093710
- [6] Herbort C, Arbelo Jorge E, and Jourdan M 2009 *Appl. Phys. Lett.* **94** 142504
- [7] Sukegawa H, Wang W, Shan R, Nakatani T, Inomata K, and Hono K 2009 *Phys. Rev. B* **79** 184418
- [8] Ebke D, Drewello V, Schäfers M, Reiss G, Thomas A 2009 *Appl. Phys. Lett.* **95** 232510
- [9] Wurmehl S, Fecher G, Kroth K, Kronast F, Dürr H A D, Takeda Y, Saitoh Y, Kobayashi K, Lin H J, Schönhense G and Felser C 2006 *J. Phys. D: Appl. Phys.* **39** 803
- [10] Miyazaki H, Soda K, Kato M, Yagi S, Takeuchi T, Nishino Y 2007 *J. Electron Spectrosc. Relat. Phenom.* **156** 347
- [11] Imada S, Yamasaki A, Kusuda K, Higashiya A, Irizawa A, Sekiyama A, Kanomatae T, Suga S 2007 *J. Electron Spectrosc. Relat. Phenom.* **156** 433
- [12] Correa J S, Eibl C, Rangelov G, Braun J, and Donath M 2006 *Phys. Rev. B* **73**, 125316
- [13] Cinchetti M, Wüstenberg J P, Sanchez Albaneda M S, Steeb F, Conca A, Jourdan M and Aeschlimann M, 2007 *J. Phys. D: Appl. Phys.* **40** 1544
- [14] Miyamoto K, Kimura A, Miura Y, Shirai M, Ye M, Cui Y, Shimada K, Namatame H, Taniguchi M, Takeda Y, Saitoh Y, Ikenaga E, Ueda S, Kobayashi K, and Kanomata T (2009) *Phys. Rev. B* **79** 100405.
- [15] Ouardi S, Balke B, Gloskovskii A, Fecher G H, Felser C, Schönhense G, Ishikawa T, Uemura T, Yamamoto M, Sukegawa H, Wang W, Inomata K, Yamashita Y, Yoshikawa H, Ueda S and Kobayashi K 2007 *J. Phys. D: Appl. Phys.* **42** 084019
- [16] Wang W H, Przybylski M, Kuch W, Chelaru L I, Wang J, Lu Y F, Barthel J, Meyerheim H L, and Kirschner J 2005 *Phys. Rev. B* **71** 144416
- [17] Fecher G H, Kandpal H C, Wurmehl S, Morais J, Lin H J, Elmers H J, Schönhense G and Felser C 2005 *J. Phys.: Condens. Matter* **17** 7237
- [18] Miura Y, Nagao K, and Shirai M 2004 *Phys. Rev. B* **69** 144413
- [19] Herbort C, Arbelo E, and Jourdan M 2009 *J. Phys. D: Appl. Phys.* **42** 084006
- [20] Jourdan M, Arbelo Jorge E, Herbort C, Kallmayer M, Klaer P, and Elmers H J 2009 *Appl. Phys. Lett.* **95** 172504
- [21] Arbelo Jorge E, Jourdan M, Kallmayer M, Klaer P, and Elmers H J 2010 *Journal of Physics: Conference Series* **200** 072006

- [22] Gewinner G, Peruchetti J C, Jaegle A, and Pinchaux R 1983 *Phys. Rev. B* **27** 3358
- [23] Habig P and Riedinger R 1990 *Vacuum* **41** 1135
- [24] Johansson L I, Petersson L G, Berggren K F, and Allen J W 1980 *Phys. Rev. B* **22** 3294
- [25] Tange A, Gao C L, Yavorsky B Y, Maznichenko I V, Etz C, Ernst A, Hergert W, Mertig I, Wulfhekel W, and Kirschner J 2010 *Phys. Rev. B* **81** 195410
- [26] Yeh J J and Lindau I 1985 *Atomic Data and Nuclear Data Tables* **32** 1
- [27] Helander M G, Greiner M T, Wang Z B, Lu Z H 2010 *Appl. Surface Science* **256** 2602
- [28] Hüfner S, 2003 *Photoelectron Spectroscopy* Springer-Verlag Berlin
- [29] Block T, Felser C, Jakob G, Enslin J, Mühling B, Gütlich P, and Cava R J 2003 *J. Solid State Chem.* **176** 646
- [30] Fecher G H, Felser C 2007 *J. Phys. D: Appl. Phys.* **40** 1582
- [31] Xu X G, Zhang D L, Wang W, Wu Y, Wang Y K, and Jiang Y 2010 *J. Magn. Mag. Mat.* **322** 3351
- [32] Chiang T C, Knapp J A, Aono M, and Eastman D E 1980 *Phys. Rev. B* **21** 3513